J Physiol (2003), **548.3**, *pp.* 691–702

DOI: 10.1113/jphysiol.2003.039198
www.jphysiol.org

Modulation of human *ether-à-go-go*-related K^+ (HERG) channel inactivation by Cs^+ and K^+

Shetuan Zhang, Steven J. Kehl and David Fedida

Department of Physiology, University of British Columbia, 2146 Health Sciences Mall, Vancouver, BC, Canada V6T 1Z3

Unlike many other native and cloned K^+ channels, human *ether-à-go-go*-related K^+ (HERG) channels show significant Cs^+ permeability with a P_{Cs}/P_K (the permeability of Cs^+ relative to that of K^+) of 0.36 ± 0.03 (n = 10). Here, we find that raising the concentration of external Cs^+ (Cs^+_o) dramatically slows HERG channel inactivation without affecting activation. Replacement of 5 mM K^+_o by 135 mM Cs^+_o increased both inactivation and recovery time constants and shifted the mid-point of the steady-state inactivation curve by 25 mV in the depolarized direction (n = 6, P < 0.01). Raising $[Cs^+]_o$ also modulated the voltage sensitivity of inactivation gating. With 130 mM Cs^+_i and 135 mM $NMDG^+_o$, the inactivation time constant decreased e-fold per 47.5 ± 1.1 mV (n = 5), and when 20 mM Cs^+ was added to the bath solution, the inactivation time constant decreased e-fold per 20.6 ± 1.3 mV (n = 5, P < 0.01). A quantitative analysis suggests that Cs^+_o binds to a site in the pore that is influenced by the transmembrane electrical field, so that Cs^+_o-induced slowing of HERG inactivation is less prominent at strong depolarizations. K^+_o has effects that are similar to Cs^+_o and their effects were additive, suggesting Cs^+_o and K^+_o may share a common mechanism of action. The strong effects of Cs^+ on inactivation but not on activation highlight the importance of ion and channel interactions during the onset of inactivation in the HERG channel.

(Resubmitted 9 January 2003; accepted after revision 7 February 2003; first published online 7 March 2003)
Corresponding author D. Fedida: Department of Physiology, University of British Columbia, 2146 Health Sciences Mall, Vancouver, BC, Canada V6T 1Z3. Email: fedida@interchange.ubc.ca

The human *ether-à-go-go*-related (*HERG*) gene encodes the pore forming subunit of a K^+ channel that exists in a number of cell types including neurons, cardiac myocytes and tumour cells (Trudeau *et al.* 1995; Faravelli *et al.* 1996; Bianchi *et al.* 1998). In the heart, HERG channels are partly responsible for a delayed rectifier K^+ current (I_{Kr}) that is important for cardiac action potential repolarization (Sanguinetti & Jurkiewicz, 1990; Sanguinetti *et al.* 1995). Reduction of I_{Kr} by mutations of the *HERG* gene or by drug block causes some congenital and acquired forms of human long-QT syndrome (Sanguinetti *et al.* 1995; Zhang *et al.* 2001).

HERG inactivation is basically C-type in nature (Trudeau *et al.* 1995; Sanguinetti *et al.* 1995; Smith *et al.* 1996; Spector *et al.* 1996), although the gating behaviour is distinctive. First, channel inactivation is much faster than voltage-dependent activation, resulting in its characteristic rectification. Second, unlike C-type inactivation in *Shaker*-type channels (Hoshi *et al.* 1991; Ogielska *et al.* 1995; Fedida *et al.* 1999), HERG inactivation displays intrinsic voltage dependence (Smith *et al.* 1996; Spector *et al.* 1996). It has been proposed that HERG channels possess a voltage sensor for inactivation (Wang *et al.* 1996; Johnson *et al.* 1999), but this has not been identified and the molecular mechanisms of HERG inactivation are not yet completely understood. C-type inactivation is known to be regulated by permeant ions, and in *Shaker* and Kv1 channels, raising the concentration of external K^+ (K^+_o) slows C-type inactivation (Lopez-Barneo *et al.* 1993), an effect that appears to be due to occupancy of the pore selectivity filter by K^+ (Baukrowitz & Yellen, 1995). Other ions, such as Cs^+, are much less effective than K^+ in their ability to modulate inactivation (Lopez-Barneo *et al.* 1993). Raising $[K^+]_o$ also slows HERG channel inactivation (Wang *et al.* 1996, 1997) but the mechanism remains poorly understood. A 'foot-in-the-door' mechanism was initially proposed to account for the slowing of deactivation of K^+ channels in the presence of external K^+ and Rb^+ (Swenson & Armstrong, 1981; Matteson & Swenson, 1986). The same mechanism was also proposed to account for the slowing of K^+ current inactivation in molluscan neurons (Ruben & Thompson, 1984) and for the slowing of C-type inactivation of *Shaker* K^+ current by external K^+ (Baukrowitz & Yellen, 1995, 1996). It is not known whether monovalent cations such as Cs^+ can affect HERG inactivation in the same way as they do in *Shaker* and Kv1 channels.

Cs^+ has been used in HERG channel studies for two major purposes. First, Cs^+ is used to block HERG channels (Trudeau *et al.* 1995; Pancrazio *et al.* 1999). Block of inward HERG current by Cs^+ is voltage dependent which is thought to reflect Cs^+ entering the pore from the outside

and interfering with K^+ permeation (Trudeau *et al.* 1995). Second, in the presence of high concentrations of external Cs^+ (Cs_o^+), large outward currents with an inactivation phase can be recorded during depolarizing pulses, in contrast to the small outward HERG currents recorded in the presence of K_o^+ (Schönherr & Heinemann, 1996; Pennefather *et al.* 1998; Barros *et al.* 1998). However, the changes of gating kinetics responsible for such large outward current with high $[Cs^+]_o$ are not known and a detailed analysis of Cs^+ effects on HERG channels has not been reported. Although the blocking properties of Cs^+ on HERG channels suggest that Cs^+ may enter the channel pore (Trudeau *et al.* 1995), the permeation of Cs^+ through HERG channels has not been studied in detail. Here, we have studied Cs_o^+ modulation of HERG channels. We found that HERG channels readily conduct Cs^+, and that high $[Cs^+]_o$ dramatically slows HERG channel inactivation but does not affect HERG activation properties. The effect of Cs_o^+ on inactivation is twofold: first, it increases the inactivation time constant (τ_{inact}) and second, it modulates the voltage sensitivity of HERG channel inactivation. A quantitative analysis of the data indicates that Cs_o^+ binding to a site located in the transmembrane electrical field can explain both effects.

METHODS

Cells and solutions

HERG currents were recorded from channels stably expressed in a human embryonic kidney cell line, HEK 293 (American Type Culture Collection, Rockville, MD, USA). Cells were maintained in Dulbecco's modified Eagle's medium plus 10% fetal bovine serum with 1% penicillin–streptomycin and G418 (0.5 mg ml^{-1}) to select for transfected cells. The pipette solution contained (mM): KCl or CsCl, 130; EGTA, 5; $MgCl_2$, 1; Hepes, 10; and was adjusted to pH 7.2 with KOH or CsOH.

The bath solution contained (mM): Hepes, 10; $MgCl_2$, 1; $CaCl_2$, 2; the balance of ions was made up with 140 mM *N*-methyl-D-glucamine ($NMDG^+$), and was adjusted to pH 7.4 with HCl. For recordings in the presence of different external Na^+, K^+, or Cs^+ concentrations, the $NMDG^+$-based external solution was used and the concentration of $NMDG^+$ was reduced as the cation concentration was elevated to maintain constant osmolarity, and the pH was adjusted to 7.4 with the appropriate hydroxide solution. All chemicals were from Sigma. Throughout the text the subscripts 'i' and 'o' denote, respectively, intra- or extracellular ion concentrations.

Electrophysiological procedures and analysis

Coverslips containing cells were removed from the incubator before experiments and placed in a superfusion chamber containing the control bath solution at 22–23 °C. The bath solution was constantly flowing through the chamber and the solution was exchanged by switching the perfusates at the inlet of the chamber, with complete bath solution changes taking 10 s. Whole-cell current recording and data analysis were performed using an Axopatch 200A amplifier and pCLAMP6 software (Axon Instruments, Foster City, CA, USA). Patch electrodes were fabricated using thin-walled borosilicate glass (World Precision Instruments, FL, USA). The electrodes had resistances of ~2 MΩ when filled with the pipette solutions. Data were filtered at 5–10 kHz and sampled at 20–50 kHz for all protocols. Typically, 80% series resistance (R_s) compensation was used. Leak subtraction was not used. Data are shown as means ± S.E.M. Statistical significance was determined using the Student's unpaired *t* test. All data analysis and curve fitting were done with Clampfit (Axon Instruments). Conductance and voltage data were fitted to a single Boltzmann function:

$$y = 1/(1 + \exp((V_{½} - V)/k)), \quad (1)$$

where y is the current normalized with respect to the maximal current, $V_{½}$ is the half-activation or inactivation potential (mid-point of the activation or inactivation curve), V is the test voltage and k is the slope factor, in millivolts, reflecting the steepness of the voltage dependence of gating.

Model of Cs_o^+ effects on HERG inactivation rate

The HERG inactivation rate is intrinsically voltage dependent. We used the following equation to describe the rate of inactivation (α):

$$\alpha(V) = \alpha_0 \times \exp(Z'\delta' FV/RT), \quad (2)$$

where $\alpha(V)$ is the inactivation rate at any voltage, α_0 is the inactivation rate at 0 mV, Z' is the valence of the charges moved by depolarization, δ' is the electrical distance from the external side of the membrane, F, R and T have their usual meanings, and RT/F is 25 mV at the room temperature at which all experiments were carried out. There is also a site at which cation binding affects inactivation. The probability that this modulatory site does not have Cs_o^+ bound is:

$$1 - \text{occupancy} = O/(O + B) = 1/(1 + ([Cs^+]/K_d(V))), \quad (3)$$

where B is the number of channels with Cs^+ bound, and O is the number of unbound channels. If the site is located within the transmembrane electrical field, the binding of cations is likely to be voltage dependent (Woodhull, 1973) such that:

$$K_d(V) = K_d(0) \times \exp(Z\delta FV/RT), \quad (4)$$

where $K_d(V)$ is the affinity at voltage V, $K_d(0)$ is the equilibrium dissociation constant at 0 mV, Z for Cs^+ or K^+ is 1 and δ is the electrical distance of the cation binding site from the external side of the membrane.

We found that, as with K_o^+, raising $[Cs^+]_o$ slowed the time course of the inactivation (see Results). The simplest explanation for this effect, which is also seen with external TEA^+ (Smith *et al.* 1996), is a gating scheme in which Cs^+ must dissociate from the modulatory site to allow inactivation (I) to proceed from the open (O) state:

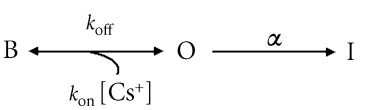

If binding and dissociation of Cs^+ are rapid (at equilibrium) relative to the rate of inactivation (α), then the apparent rate of inactivation will be:

$$\alpha(V,Cs) = \alpha(V) \times (O/(O + B)) = \alpha(V) \times (1/(1 + ([Cs^+]/K_d(V)))),$$

$$\alpha(V,Cs) = (\alpha_0 \times \exp(Z'\delta' FV/RT)) \times (1/(1 + ([Cs^+]/(K_d(0) \times \exp(Z\delta FV/RT))))), \quad (5)$$

where the equilibrium dissociation constant, K_d, is equal to k_{off}/k_{on}; $\alpha(V,Cs)$ is the inactivation rate in the presence of Cs^+ at voltage V

and $\alpha(V)$ is the inactivation rate in the absence of Cs^+ at voltage V. $\alpha(V,Cs)$ is thus a function of both voltage (V) and Cs^+ concentration $[Cs^+]_o$. We assumed a 1:1 stoichiometry for the interaction between the channel and Cs^+_o.

It should be noted that $Z'\delta'$ is the apparent charge associated with the intrinsic inactivation rate in the absence of external Cs^+ and K^+, and $Z\delta$ is the apparent charge in the presence of external Cs^+ or K^+. Thus, α_0 and $Z'\delta'$ are the 'external ion-independent' components. The values for α_0 are measured experimentally. $Z'\delta'$ was considered a single parameter and obtained from fitting the τ_{inact}–voltage relationship in the absence of Cs^+_o or K^+_o. These numbers were then constrained to be the same at all concentrations of Cs^+_o or K^+_o. It should also be noted that eqn (5) does not predict perfectly linear relationships between $\log(\tau_{inact})$ and voltage (V), and the curvature can be seen in Fig. 7*C* and *D* especially for concentrations near the $K_d(0)$. Since HERG steady-state inactivation is nearly complete at positive voltages at which the time constant for inactivation (τ_{inact}) was measured in the present study, the τ_{inact} is considered the reciprocal of $\alpha(V,Cs)$, and is used throughout the text and figures.

RESULTS

External Cs^+ modifies HERG current

Figure 1*A* shows typical HERG currents in 130 mM K^+_i and 5 mM K^+_o, elicited by 4 s depolarizing steps from the holding potential of −80 mV to between −70 and +70 mV. Tail current peak amplitudes were measured during the subsequent step to −50 mV where the inactivated channels recover quickly to the open state and then slowly deactivate (Trudeau *et al.* 1995; Sanguinetti *et al.* 1995; Smith *et al.* 1996; Spector *et al.* 1996). The current–voltage (I–V) relationship for HERG peak outward current measured during the depolarizing steps is shown as open circles in Fig. 1*C* and the normalized tail current peak amplitude at −50 mV *versus* depolarizing voltage is shown as open triangles in Fig. 1*D*. HERG current activated at voltages positive to −50 mV, maximum current was reached for steps to −10 mV and at more positive voltages inward rectification resulted from rapid voltage-

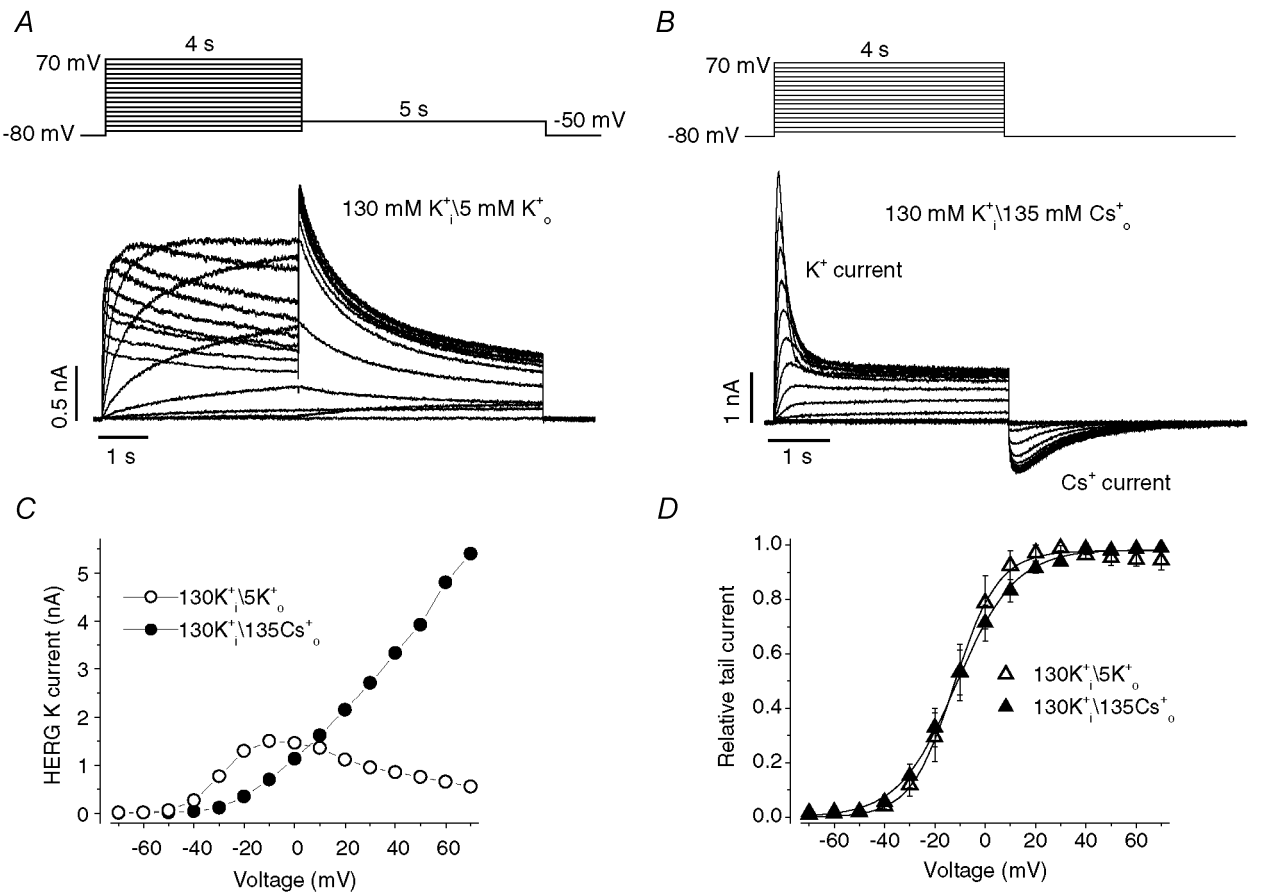

Figure 1. External Cs^+ modifies human *ether-à-go-go*-related K^+ (HERG) current inactivation

A and *B*, families of HERG currents elicited by the voltage protocol (10 mV steps) shown above the current traces in external solution containing 5 mM K^+_o (*A*) or 135 mM Cs^+_o (*B*) with an internal solution containing 130 mM K^+_i. *C*, current–voltage (I–V) relationships for peak outward HERG current during depolarizing pulses in *A* (○) and *B* (●). *D*, voltage dependence of HERG activation. Amplitudes of tail currents were normalized to the largest current and plotted *versus* prepulse potentials. The normalized data for each cell were fitted to a Boltzmann function. The averaged half-activation voltage ($V_{½}$) and the slope factor (k) in 5 mM K^+_o are, respectively, −11.1 ± 4.0 mV and 7.9 ± 0.7 mV (n = 4). The corresponding values in 135 mM Cs^+_o solution are −9.8 ± 3.5 mV and 9.3 ± 0.4 mV (n = 6).

dependent inactivation (Smith *et al.* 1996; Spector *et al.* 1996; Zhang *et al.* 1999). The tail currents reached a saturating amplitude following voltage steps positive to 20 mV.

Replacement of 5 mM K_o^+ by 135 mM Cs_o^+ resulted in an increase of outward K^+ currents that inactivated quickly as previously reported (Schönherr & Heinemann, 1996). In Fig. 1*B*, HERG currents were elicited by depolarizing steps to between −70 and +70 mV for 4 s. HERG channels displayed a significant Cs^+ conductance, with visible inward Cs^+ tail currents upon repolarization to −80 mV. The *I–V* relationship for maximal HERG current measured during depolarizing steps is shown as filled circles in Fig. 1*C*, and the normalized tail current peak amplitude at −80 mV *versus* the depolarizing voltage used to activate the current is shown as filled triangles in Fig. 1*D*. In 135 mM Cs_o^+, the relationship between the peak outward current and voltage was no longer bell-shaped but showed a monotonic increase with depolarizing potential (Fig. 1*C*). Despite this dramatic change of the *I–V* relationship, the voltage dependence of HERG channel activation in solutions with 5 mM K_o^+ and 135 mM Cs_o^+ was found to be similar (Fig. 1*D*). Therefore, although replacement of 5 mM K_o^+ by 135 mM Cs_o^+ affected the peak *I–V* relationship, this was not the result of an action on the voltage dependence of HERG channel activation.

Cs^+ readily permeates HERG channels

From the inward tail currents in Fig. 1*B*, it is clear that Cs^+ permeates HERG channels. We studied the permeability of Cs^+ relative to that of K^+ (P_{Cs}/P_K) by determining reversal potentials under bi-ionic conditions in which 135 mM K^+ was present on one side and 135 mM Cs^+ was present on the other side of the membrane. Fully activated HERG open channel instantaneous *I–V* relationships derived with the protocol shown in Fig. 2*A* were plotted, and reversal potentials were obtained. The P_{Cs}/P_K was then calculated (Hille, 2001). We found that $P_{Cs,out}/P_{K,in}$ was 0.34 ± 0.03 ($n = 6$) and $P_{Cs,in}/P_{K,out}$ was 0.38 ± 0.04 ($P > 0.05$, $n = 4$). There is apparently no preferential direction for Cs^+ to permeate the channel, and the pooled data give a P_{Cs}/P_K of 0.36 ± 0.03 ($n = 10$). To compare the conduction properties of Cs^+ and K^+ current through HERG channels, *I–V* relationships were obtained in either symmetrical Cs^+ or K^+ conditions (Fig. 2). The *I–V* relationships are nearly linear to +80 mV under both conditions. The slope conductance of the linear fit to the relationships in symmetrical Cs^+ or K^+ was 1.23 ± 0.17 and 3.66 ± 0.77 nS pF^{-1}, respectively.

High Cs_o^+ does not affect HERG activation kinetics

The enhanced peak outward current in 135 mM Cs_o^+ (Fig. 1*B* and *C*) was not due to an increased driving force because the reversal potential in 130 mM K_i^+ and 135 mM Cs_o^+ was more positive (−28.3 ± 2.4 mV, $n = 6$) than that with 130 mM K_i^+ and 5 mM K_o^+ (−81.2 ± 2.9 mV, $n = 4$). The instantaneous *I–V* relationship also gave no indication of impaired outward K^+ current (Fig. 2). Thus, enhanced outward K^+ current recorded with 135 mM Cs_o^+ may result either from an acceleration of activation and/or a slowing of inactivation. We therefore studied the activation time course in solutions containing either 5 mM K_o^+ or 135 mM Cs_o^+ (Fig. 3). Activation time constants (τ_{act}) were determined by fitting the envelope of the extrapolated (see below) peak amplitudes of tail current recorded at repolarizing steps to −50 mV after varying

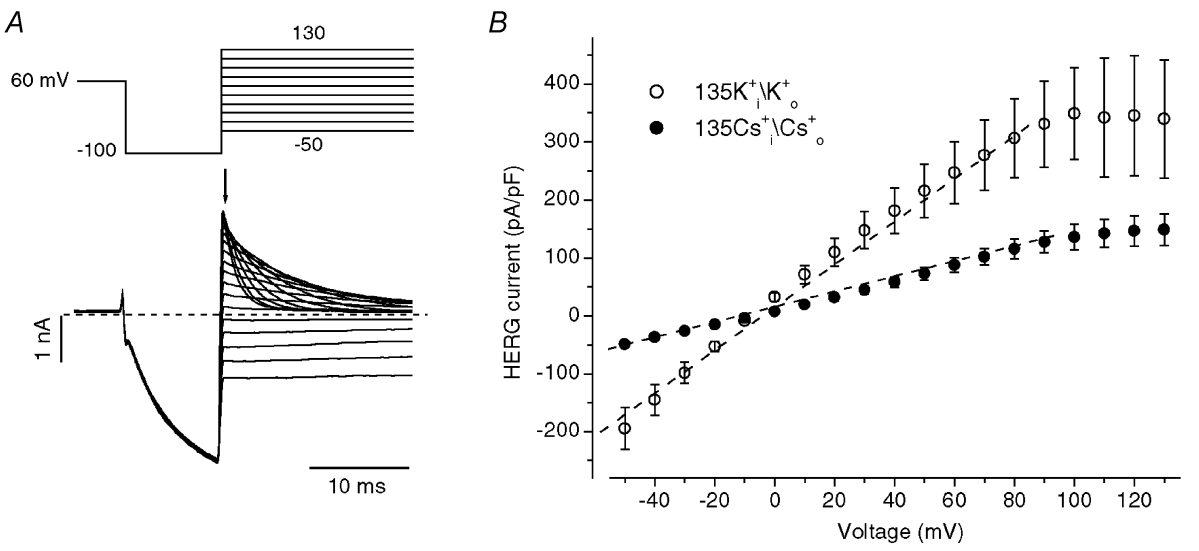

Figure 2. The HERG channels conduct K^+ better than Cs^+

A, HERG currents elicited by the voltage protocol above the current traces in symmetrical 135 mM K^+. *B*, fully activated HERG open channel (instantaneous, signified by the arrow in *A*) current–voltage relationships in either symmetrical K^+ (○) or Cs^+ (●). The conductance was determined from the slope of a linear fit to current amplitudes at potentials between −50 and +80 mV.

duration depolarizations to between −20 and +80 mV from a holding potential of −80 mV. During the subsequent step to −50 mV, HERG channels reopen (recover from inactivation) much faster than they close (deactivate). Consequently, the tail current rises to a peak and then decays. Thus, deactivation overlaps recovery from inactivation. To estimate the peak current amplitude immediately (time 0) following repolarization, the deactivating phase of tail current for each trace was fitted to a single exponential function and extrapolated to time 0 of repolarization. The current amplitude at time 0, which is assumed to be proportional to the total number of activated channels, is plotted against the depolarizing duration and fitted to a single exponential function to obtain the time constant of activation. It should be noted that because HERG activation is sigmoidal in nature, the fit to a single exponential function represents a simplified approximation. Data in Fig. 3*A* and *B* show the original tail current traces obtained after 60 mV depolarizing steps in external solution containing 5 mM K^+ and 135 mM Cs^+, respectively. The extrapolated peak tail currents from Fig. 3*A* (■) and *B* (●), and single exponential fits to them (continuous lines) are shown in Fig. 3*C*. The values for τ_{act} were similar in 5 mM K^+_o or 135 mM Cs^+_o. The voltage dependences of τ_{act} in 5 mM K^+_o (■) or 135 mM Cs^+_o (●) are plotted in Fig. 3*D*. It can be seen that there is little difference in the macroscopic activation rate of HERG current in external solutions containing either 5 mM K^+ or 135 mM Cs^+.

High $[Cs^+]_o$ slows HERG inactivation

We next studied the effects of replacement of 5 mM K^+_o by 135 mM Cs^+_o on HERG channel inactivation and discovered that 135 mM Cs^+_o slowed HERG current inactivation. To measure the inactivation time constant (τ_{inact}), we used the protocol shown above the current traces in panel *A* of Fig. 4. HERG current was fully activated and inactivated at the holding potential of +60 mV. The cell was then repolarized to −100 mV for 10 ms to allow recovery from inactivation and to minimize deactivation of HERG channels (Smith *et al.* 1996; Spector *et al.* 1996). A test step was then applied to different voltages to observe the inactivation time course. The τ_{inact} was obtained by fitting the currents to a single exponential function. Data in Fig. 4*A* and *B* show HERG current traces in external solutions containing 5 mM K^+_o (*A*) or 135 mM Cs^+_o (*B*). The averaged τ_{inact} in 5 mM K^+_o (○) and 135 mM Cs^+_o (●) in nine cells are plotted as a function of test potential in Fig. 4*E*. A concentration of 135 mM Cs^+_o slowed HERG inactivation at all voltages tested. For example, τ_{inact} at 0 mV increased from 10.1 ± 0.1 ms in 5 mM K^+_o to 66.4 ± 4.8 ms in 135 mM Cs^+_o ($n = 9$, $P < 0.01$).

The effects of replacement of 5 mM K^+_o by 135 mM Cs^+_o on HERG channel recovery from inactivation were also examined. As shown above Fig. 4*C*, the voltage protocol consisted of a depolarization to 60 mV for 400 ms to inactivate HERG channels, followed by repolarization to potentials between −150 and −10 mV to elicit a tail current. The rising phase of the tail current represents the rapid recovery of HERG channels from inactivated to open state and is followed by channel deactivation. The current traces were fitted to a single (increasing phase, > −80 mV) or double exponential function (increasing and decreasing phases, ⩽ −80 mV), and the time constant for recovery (τ_{rec}) was obtained (Sanguinetti *et al.* 1995;

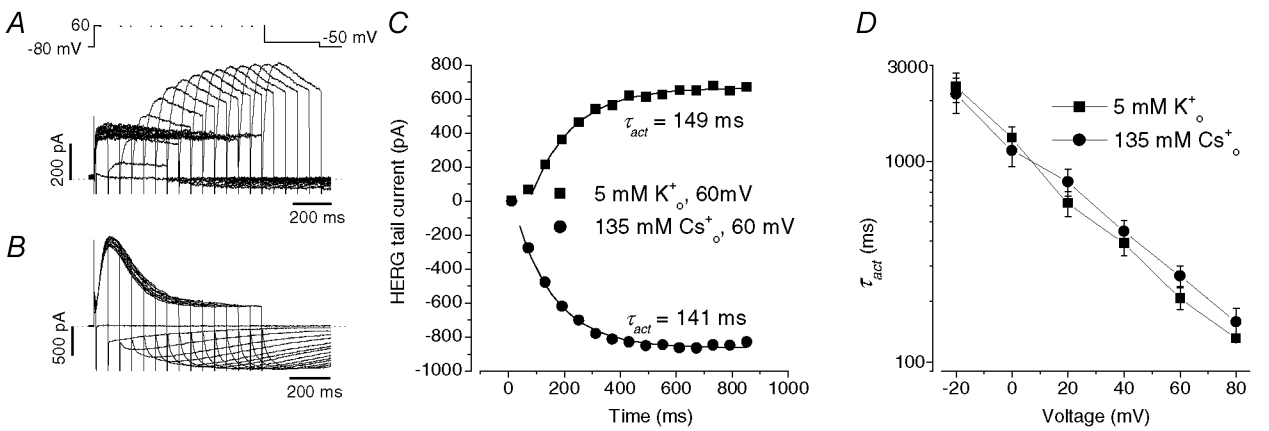

Figure 3. HERG current activation is similar in 5 mM K^+_o and 135 mM Cs^+_o

The values for activation time constants (τ_{act}) were determined by fitting the envelopes of the extrapolated peak amplitude of tail currents recorded at −50 mV after varying duration depolarizations to between −20 and +80 mV from a holding potential of −80 mV. The protocol for a depolarization to +60 mV is shown above panel *A*. The internal solution contained 130 mM K^+. *A* and *B* show envelopes of tail currents elicited by a depolarization to 60 mV with variable duration in external solution containing 5 mM K^+_o (*A*) or 135 mM Cs^+_o (*B*). *C*, τ_{act} was measured from single exponential fits to the extrapolated peak tail current envelope from *A* (■) and *B* (●). The values for τ_{act} were 149 and 141 ms, respectively. *D*, the voltage dependence of τ_{act} in external solution containing 5 mM K^+_o (■) or 135 mM Cs^+_o (●) (n = 5–8).

Spector *et al.* 1996). Replacement of 5 mM K^+_o (Fig. 4*C*) by 135 mM Cs^+_o (Fig. 4*D*) significantly slowed the recovery from inactivation ($P < 0.01$, $n = 8$). Thus, 135 mM Cs^+_o slows the time course of both inactivation and recovery from inactivation.

To study the effects of replacement of 5 mM K^+_o by 135 mM Cs^+_o on the voltage dependence of steady-state inactivation, a triple-pulse protocol was used (Fig. 5). After a 500 ms pulse to + 60 mV to activate and then inactivate HERG channels, a pulse to −100 mV was applied for 20 ms to allow channels to recover from inactivation. The third pulse (P3) consisted of steps to potentials between from −100 mV to + 90 mV to record the voltage dependence of current inactivation. Following the approach of Wang *et al.* (1997), the steady-state inactivation relationship was calculated as the ratio of the currents measured at 100 ms to the instantaneous current of P3. The ratio was normalized to the maximal value, plotted against the P3 voltage and fitted to a Boltzmann function (Fig. 5). Replacement of 5 mM K^+_o with 135 mM Cs^+_o shifted the mid-point of the steady-state inactivation curve to more positive potentials by 25 mV ($n = 6$, $P < 0.01$) and decreased the slope factor from 15.8 ± 1.2 mV to 12.8 ± 0.7 mV ($n = 6$, $P < 0.05$).

Concentration dependence of Cs^+_o and K^+_o effects on HERG inactivation

The effect of Cs^+_o on the voltage dependence of HERG τ_{inact} was concentration dependent (Fig. 6*A*). The voltage dependence of HERG τ_{inact} at different $[Cs^+]_o$ is plotted in panel *A*. Cs^+_o not only increased τ_{inact} but also modulated the voltage sensitivity. When $\log_{10}\tau_{inact}$ −*V* was fitted to a linear function, it was found that the τ_{inact} decreased e-fold per 51.5 ± 1.3 mV ($n = 9$), 49.1 ± 1.0 mV ($P > 0.05$, $n = 5$), 39.3 ± 0.4 mV ($P < 0.01$, $n = 6$), 36.3 ± 0.6 mV ($P < 0.01$, $n = 9$), 36.2 ± 1.4 mV ($P < 0.01$, $n = 6$) and 35.7 ± 0.8 mV ($P < 0.01$, $n = 9$) at 0, 1, 5, 20, 67.5 and 135 mM Cs^+_o, respectively (one-way ANOVA, compared to that in zero Cs^+_o). To get insight into the effects of Cs^+_o, we used a gating scheme in which Cs^+_o-bound channel cannot inactivate, and used eqn (3) to describe the concentration dependence of Cs^+_o binding to the channel (Methods). We reasoned that if the binding site is located in the membrane electrical field, the K_d would also be voltage dependent (Woodhull, 1973). Since HERG channel inactivation is intrinsically voltage dependent, HERG inactivation rate is a function of both voltage and Cs^+_o concentrations (see Methods for details). Continuous lines superimposed on the data represent the least squares fit of eqn (5) (Methods)

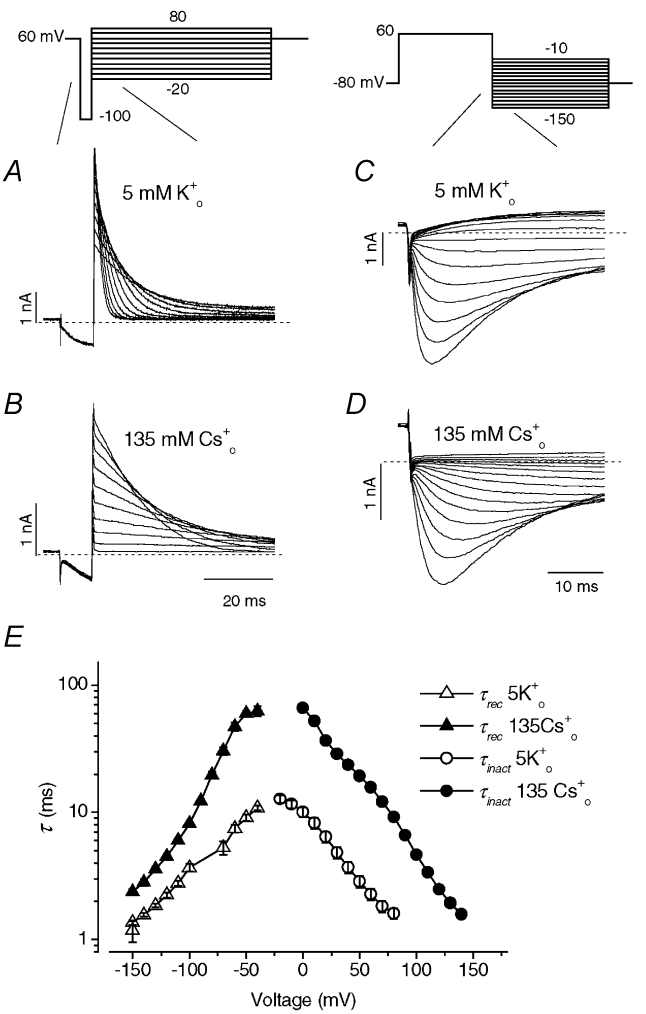

Figure 4. 135 mM Cs^+_o slows both onset of and recovery from HERG inactivation

A and *B*, HERG currents elicited by the voltage protocol shown above the current traces in external solution containing 5 mM K^+_o (*A*) or 135 mM Cs^+_o (*B*) with an internal solution containing 130 mM K^+. Starting from a holding potential of +60 mV, a 10 ms repolarizing step to −100 mV allowed HERG channels to recover from inactivation, and steps to a range of test potentials allowed the inactivation time course to be observed. Current traces represent responses in the time interval demarcated by the slanted lines in the voltage protocol. *C* and *D*, the time and voltage dependence of recovery from inactivation was measured by the voltage protocol shown above the current traces in external solution containing 5 mM K^+_o (*C*) or 135 mM Cs^+_o (*D*) and with 130 mM K^+_i. HERG was activated by a 400 ms pulse to 60 mV, followed by a test pulse to different potentials to record HERG tail currents. The time constant of recovery (τ_{rec}) from inactivation was measured as the single exponential fit to the rising phase (> −80 mV) or as the fast time constant of a double exponential fit (⩽ −80 mV) to HERG tail current (Sanguinetti *et al.* 1995; Spector *et al.* 1996). *E*, voltage dependence of the τ_{rec} and the inactivation time constant (τ_{inact}) in external solution containing 5 mM K^+_o (△, ○) or 135 mM Cs^+_o (▲, ●). Each point is the mean ± S.E.M. for eight to nine cells.

Table 1. Free parameters in the fitting of the effects of $[Cs^+]_o$ and $[K^+]_o$ on the voltage dependence of outward K^+ and Cs^+ current inactivation time constants

Internal solution (mM)	Cs_o^+		K_o^+		Concentration (mM)
	$K_d(0)$ (mM)	δ	$K_d(0)$ (mM)	δ	
130 K^+	5.2	0.15	10.9	0.20	1
	4.6	0.16	6.1	0.23	5
	5.6	0.15	5.1	0.24	20
	10.7	0.14	7.7	0.25	67.5
	12.8	0.14	13.5	0.25	135
130 Cs^+	1.9	0.58	1.4	0.68	1
	1.2	0.75	5.2	0.60	5
	2.1	0.75	5.7	0.53	20
	1.7	0.58	14.9	0.71	135

$K_d(0)$ is the equilibrium dissociation constant at 0 mV; δ is the electrical distance of the cation binding site from the external side of the membrane.

which combined the extracellular cation concentration- and voltage-dependent binding. The α_0 was obtained experimentally and $Z'\delta'$ was considered a single parameter and was obtained by fitting data in the absence of Cs_o^+. The values for α_0 and $Z'\delta'$ were 0.177 ms^{-1} and 0.5, respectively, and were fixed in fittings of the data at the different Cs_o^+ concentrations with eqn (5). Each fitting gave similar values for $K_d(0)$ and δ (Table 1). The means for $K_d(0)$ and δ were 7.8 ± 1.7 mM and 0.16 ± 0.01, respectively (based on the fits at five different $[Cs^+]_o$, 5–9 cells at each Cs_o^+ concentration).

Since increasing $[K^+]_o$ has also been reported (Wang *et al.* 1996, 1997) to slow HERG channel inactivation, the concentration dependence of K_o^+ effects was also studied (Fig. 6*B*). K_o^+ had very similar effects to Cs_o^+: it increased τ_{inact} and decreased voltages required per e-fold change of τ_{inact} (data not shown). Fitting data at the different $[K^+]_o$ to eqn (5) with the fixed α_0 and $Z'\delta'$ values gave similar $K_d(0)$ and δ values at each K_o^+ concentration (Table 1). The mean $K_d(0)$ and δ values were 8.7 ± 1.5 mM and 0.23 ± 0.01, respectively (based on fits at five different $[K^+]_o$, 5–11 cells at each K_o^+ concentration). The similar δ values with both

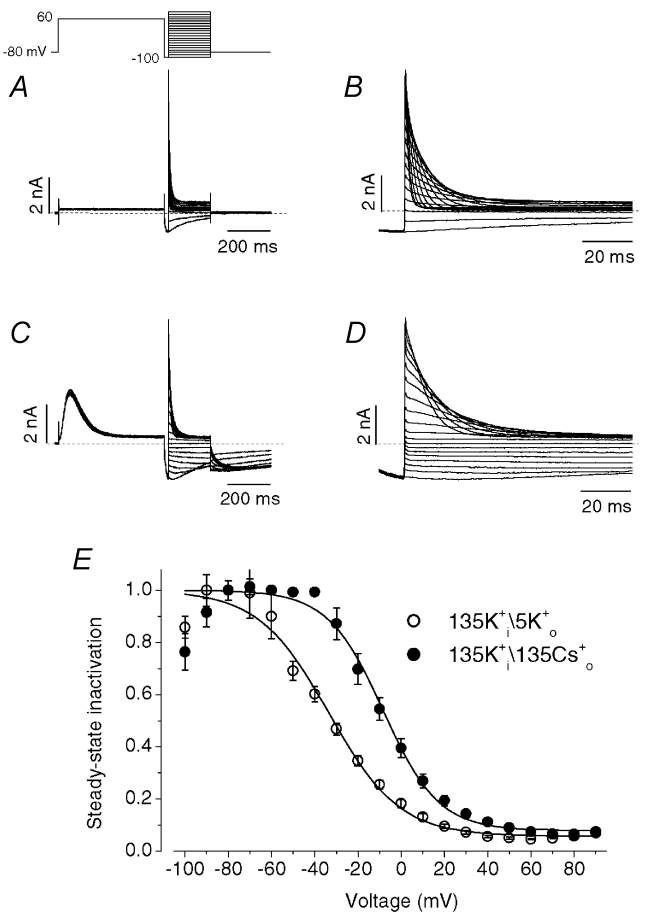

Figure 5. Replacement of 5 mM K_o^+ by 135 mM Cs_o^+ shifted the steady-state inactivation curve to more positive potentials

Steady-state inactivation was measured using a triple-pulse protocol, shown above the current traces, in bath solutions containing 5 mM K^+ (*A* and *B*) or 135 mM Cs^+ (*C* and *D*) and with 130 mM K_i^+. A 500 ms pulse (P1) to 60 mV to activate and then inactivate HERG was followed by a 20 ms pulse (P2) to −100 ms to remove the inactivation. In the third pulse (P3) the potential varied between −100 and +90 mV. Currents during the P3 pulses of *A* and *C* are expanded in *B* and *D*, respectively, to show the time course of inactivation. *E*, the steady-state inactivation was calculated as the ratio of the current measured 100 ms after the onset of P3 to the instantaneous current at the same potential in 5 mM K^+ (○) or 135 mM Cs^+ (●). The ratio was normalized to the maximal value, plotted as a function of voltage and fitted to a Boltzmann function. Such measurement represents an estimation of steady-state inactivation because of the overlapping deactivation at negative voltages. Data were obtained from six cells. The half-inactivation voltage and slope factor were −33.5 ± 2.5 mV and −15.8 ± 1.2 mV for 5 mM K_o^+, and −8.3 ± 2.6 mV and −12.8 ± 0.7 mV for 135 mM Cs_o^+, respectively. Both the change of half-inactivation voltage and slope factor are significant ($n = 6$, $P < 0.01$ and $P < 0.05$, respectively).

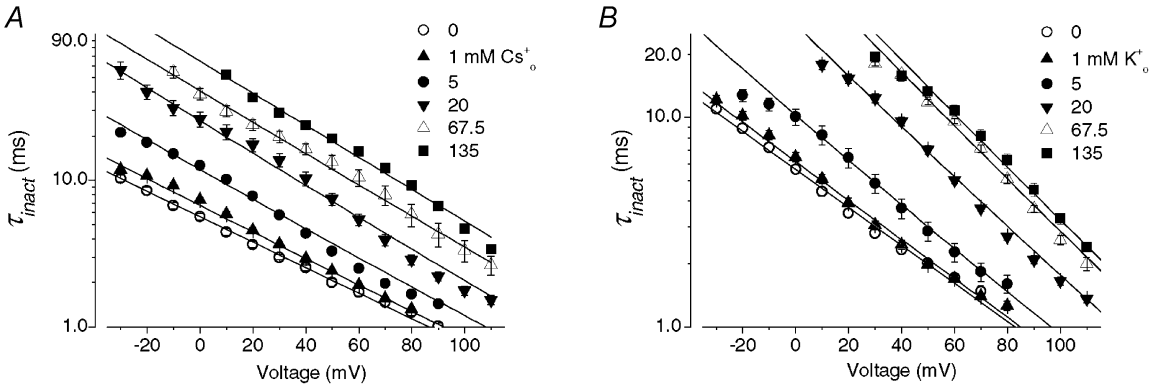

Figure 6. The effects of $[Cs^+]_o$ and $[K^+]_o$ on the voltage dependence of τ_{inact}

A, the voltage dependence of τ_{inact} with the indicated $[Cs^+]_o$ and 130 mM K^+_i is plotted. Continuous lines represent fits of the data to a model (see Methods, eqn (5)) in which binding is voltage dependent. The free parameters for each fit are shown in Table 1. The mean $K_d(0)$ and δ values are 7.8 ± 1.7 mM and 0.16 ± 0.01, respectively (n = 5). *B*, as for *A*, but with changes of $[K^+]_o$. The mean $K_d(0)$ and δ values of 8.7 ± 1.5 mM and 0.23 ± 0.01, respectively (n = 5), with K^+_o are similar to those obtained for Cs^+_o.

Cs^+_o and K^+_o suggest that they may bind to the same depth within the membrane electric field.

Voltage- and ion-dependent modulation of HERG Cs^+_o conductance

Unlike many other K^+ channels, HERG channels conduct Cs^+ readily even in the presence of K^+ (Figs 1*B* and 2). We also studied the voltage- and concentration-dependent effects of the extracellular cations on the HERG currents when outward current was carried by Cs^+ ions. To do this we used a pipette solution containing 130 mM Cs^+. By comparing current relaxations in panels *A* and *B* of Fig. 7 it can be seen that raising Cs^+_o slows inactivation of outward Cs^+ currents significantly. The concentration dependent slowing of the inactivation rate and the change of slope of the τ_{inact}–V relationships are similar to those observed for K^+ currents (Figs 4 and 6). The τ_{inact}–V curve is shown at different $[Cs^+]_o$ in Fig. 7*C*. Cs^+_o increased τ_{inact} and modulated the voltage sensitivity. When $\log_{10}\tau_{inact}$–V was fitted to a linear function, it was found that the τ_{inact}

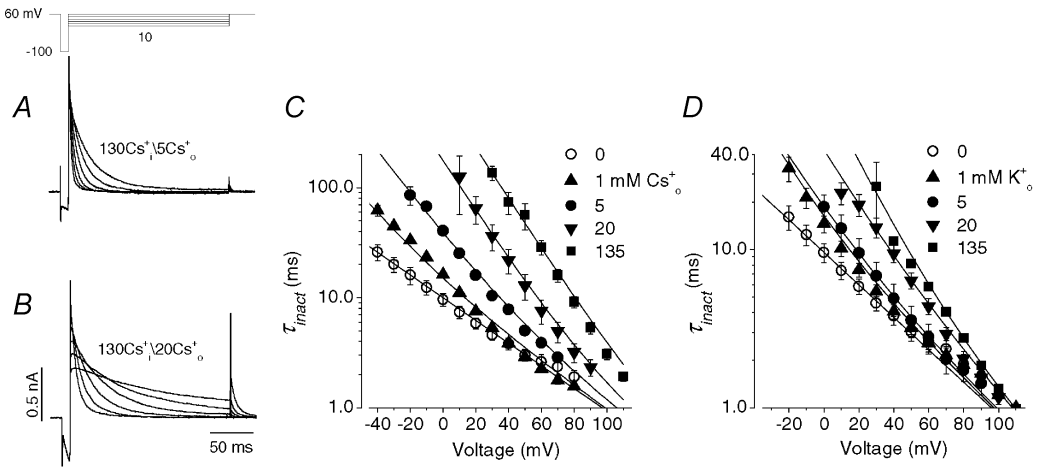

Figure 7. The effects of $[Cs^+]_o$ and $[K^+]_o$ on the voltage dependence of τ_{inact} of outward Cs^+ current recorded with 130 mM Cs^+_i

A and *B*, HERG Cs^+ currents elicited by the voltage protocol shown above the current traces in external solution containing 5 mM Cs^+_o (*A*) or 20 mM Cs^+_o (*B*). HERG channels were initially inactivated at the holding potential of +60 mV. As with data in Fig. 4, a 10 ms repolarizing step to −100 mV allows HERG channels to recover from inactivation, and steps to a range of test potentials allows the inactivation time course to be observed. *C*, voltage dependence of time constant of the decay of outward Cs^+ current at different $[Cs^+]_o$. Data were fitted (continuous lines) to eqn (5). Cs^+_o increased τ_{inact} and modulated the voltage sensitivity of the τ_{inact}–V relationship. The free parameters for each fit are shown in Table 1. The mean $K_d(0)$ and δ values are 1.7 ± 0.2 mM and 0.66 ± 0.05, respectively (n = 4). *D*, as in *C*, but with varying $[K^+]_o$. The mean $K_d(0)$ and δ values are 6.8 ± 2.8 mM and 0.63 ± 0.04, respectively (n = 4). Thus, with Cs^+_o and K^+_o the location of the binding site in the electrical field is similar but the affinity of the site for K^+ is slightly lower.

decreased e-fold per 47.5 ± 1.2 mV (n = 5), 31.2 ± 1.2 mV ($P < 0.01$, $n = 7$), 24.7 ± 0.6 mV ($P < 0.01$, $n = 6$), 20.6 ± 1.3 mV ($P < 0.01$, $n = 5$) and 20.6 ± 0.2 mV ($P < 0.01$, $n = 7$) at 0, 1, 5, 20 and 135 mM Cs^+_o, respectively (one-way ANOVA, compared to that in zero Cs^+_o). Although we fitted the $\log_{10}\tau_{inact}$–V relationship to a linear function to address the change of the voltage dependence of HERG channel inactivation, a careful inspection of the τ_{inact}–V relationship in Fig. 7*C* and *D* reveals that it is not perfectly linear especially for $[Cs^+]_o$ and $[K^+]_o$ at 5 mM. This slight non-linearity is consistent with our model described in eqn (5) which contains two exponential components, and so does not predict perfectly linear relationships between $\log_{10}\tau_{inact}$ and voltage, especially for concentrations near the $K_d(0)$. In Fig. 7*C*, the data were fitted to eqn (5). The 'external ion-independent' components α_0 and $Z'\delta'$ of 0.104 ms^{-1} and 0.6, respectively, were obtained as for K^+ current, and these values were fixed in fitting data at the different $[Cs^+]_o$ (Fig. 7*C*), as well as $[K^+]_o$ (Fig. 7*D*). The continuous lines represent the least squares fits and the number of free parameters is summarized in Table 1. The mean $K_d(0)$ and δ values were 1.7 ± 0.2 mM and 0.66 ± 0.05, respectively (based on fits at four different $[Cs^+]_o$, 5–7 cells at each concentration). For comparison, the concentration dependence of K^+_o effects was also studied (Fig. 7*D*, Table 1). The means for $K_d(0)$ and δ were 6.8 ± 2.8 mM and 0.63 ± 0.04, respectively (based on fits at four different $[K^+]_o$, 5–7 cells at each concentration). Interestingly, although the model provides good fits to experimental data under both K^+ (Fig. 6) and Cs^+ permeating conditions (Fig. 7), the δ value is apparently greater (deeper, relative to the external surface, within the electric field) when the channels are conducting Cs^+. Thus, our results showed that there are clear differences in gating kinetics when Cs^+ or K^+ is carrying the current. The model incorporated the differences in gating kinetics between Cs^+- and K^+-mediated current in terms of different δ values.

Effects of Cs^+_o and K^+_o on HERG inactivation are additive

Under the two different experimental conditions used to record outward K^+ or Cs^+ current we have shown that raising Cs^+_o or K^+_o has similar effects on HERG channel inactivation. Model analyses suggest similar $K_d(0)$ and δ values for the two ions when the major internal cation is K^+, and similar δ values when the major internal cation is Cs^+. These observations support the idea that both ions, when added extracellularly, act through a common binding site. This idea was tested using the experiment illustrated in Fig. 8, which essentially tested whether the voltage dependent actions of Cs^+_o and K^+_o were additive. Concentrations of Cs^+_o or K^+_o near $K_d(0)$ were used. In Fig. 8, the τ_{inact}–V relationships at 0 (○), 10 mM K^+_o (●), 10 mM K^+_o plus 10 mM Cs^+_o (■) were plotted. Data obtained with 20 mM K^+_o (△) and 20 mM Cs^+_o (▽) are also shown. 10 mM K^+_o increased τ_{inact}. An additional increase was caused by 10 mM K^+_o plus 10 mM Cs^+_o, which was significant ($P < 0.01$). The increase caused by 10 mM K^+_o plus 10 mM Cs^+_o is not different from that induced by either 20 mM K^+_o or 20 mM Cs^+_o ($P > 0.05$), suggesting the effects of Cs^+_o and K^+_o were additive.

DISCUSSION

Selective effect of high $[Cs^+]_o$ and $[K^+]_o$ on inactivation

Raising Cs^+_o (or K^+_o) significantly slows HERG channel inactivation, and the concentration- and voltage-dependent effects can be well expressed in terms of binding to a site located within the membrane electric field. Changing from 5 mM K^+_o to 135 mM Cs^+_o slowed both onset of and recovery from inactivation, shifted the mid-point of the steady-state inactivation by 25 mV, but did not affect either the steady-state voltage dependence or the kinetics of HERG activation (Figs 1 and 2). Our finding highlights the importance of interactions between extracellular permeant cations and the channel during the onset of inactivation in the HERG channel.

Modulation of inactivation by extracellular cations

Slowing of HERG inactivation by K^+_o has been noted previously, but the mechanism remains poorly understood (Wang *et al.* 1996, 1997). The marked effect of Cs^+_o on HERG inactivation is surprising because Cs^+_o has a much smaller effect on C-type inactivation in N-type

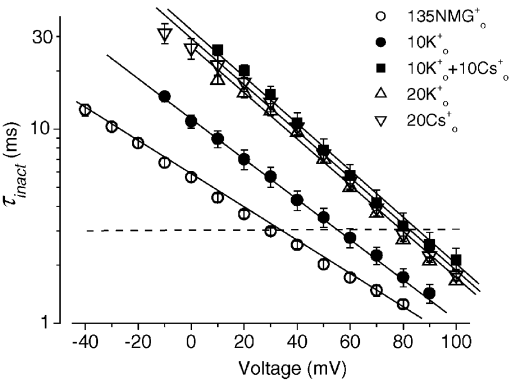

Figure 8. Effects of Cs^+_o and K^+_o on HERG inactivation were additive

Voltage dependence of K^+ current τ_{inact} with 130 mM K^+_i and 0 (○), 10 mM K^+_o (●), and 10 mM K^+_o plus 10 mM Cs^+_o (■). Data with 20 mM K^+_o (△) and 20 mM Cs^+_o (▽) (taken from Fig. 6) are also shown for comparison. When viewed as a voltage shift, at τ_{inact} of 3 ms, 10 mM K^+_o shifted the τ_{inact}–V relationship to the right by 24.2 ± 1.7 mV ($n = 6$). 10 mM K^+_o plus 10 mM Cs^+_o shifted the relationship to the right by 51.1 ± 4.4 mV ($n = 6$), which is significantly greater than the 10 mM K^+_o-induced shift ($P < 0.01$), but not different from either 20 mM K^+_o- or 20 mM Cs^+_o-induced shifts (46.0 ± 2.1, $n = 5$ and 49.2 ± 2.7 mV, $n = 9$, respectively. $P > 0.05$). This indicates that Cs^+_o and K^+_o may share a common mechanism of action.

inactivation-removed *Shaker* channels (Lopez-Barneo *et al.* 1993). We found that Cs_o^+, K_o^+ and Rb_o^+ (data not shown) all slow HERG inactivation to a similar extent and our analyses showed similar $K_d(0)$ values for Cs_o^+ and K_o^+ when the major internal cation is K^+ (Fig. 6). Compared with Cs_o^+ and K_o^+, we found that Na_o^+ had little effect on HERG inactivation (data not shown, see also Numaguchi *et al.* 2000). These results suggest that the external cation binding site selects strongly against the smaller Na^+ ion, but only modestly among the three larger ions.

The 'foot-in-the-door' mechanism was originally proposed to account for the slowing by K^+ and Rb^+ of K^+ channel deactivation in the squid giant axon and was extended to account for the effects on inactivation in K^+ channels (Swenson & Armstrong, 1981; Ruben & Thompson, 1984; Matteson & Swenson, 1986; Baukrowitz & Yellen, 1995, 1996). Slowing of HERG inactivation by external TEA^+ has also been explained by the same mechanism (Smith *et al.* 1996). In the present study, we applied the 'foot-in-the-door' concept to a model to account for the slowing of HERG channel inactivation by Cs_o^+ and K_o^+. We also reasoned that if the binding site is located in the membrane electrical field, the K_d would also be voltage dependent (Woodhull, 1973) and therefore we incorporated voltage dependent cation binding in the model. Although similar $K_d(0)$ and δ values (≈ 0.2) for Cs_o^+ and K_o^+ were obtained when the major intracellular cation was K^+ (Fig. 6), a different response to Cs_o^+ and K_o^+ was seen when the major intracellular cation was Cs^+ such that extracellular regulation site was 'deeper' ($\Delta \approx 0.6$) with Cs_i^+. When $\log_{10}\tau_{inact}$–V relationships were fitted to a linear function, Cs_o^+ has a bigger effect on the slope factor with internal Cs^+ than with internal K^+. Thus, our model incorporates the different effects by Cs_o^+ on the slope factor with internal Cs^+ *vs.* K^+ by way of different δ values. The mechanistic basis for the different δ is uncertain. Because the K^+ channel is a multi-ion pore, the δ value from a Woodhull (1973) model could be complicated by interactions between ions. The change in the apparent δ may simply result from differences in cation binding sites within the channel between K^+ and Cs^+ (in the KcsA channel, four binding sites for K^+ *vs.* three binding sites for Cs^+; Zhou & MacKinnon, 2002), and the coupling of charge movement (Spassova & Lu, 1999). Another possibility is that when physically bigger Cs^+ permeates the channel, binding of ions of different sizes at sites deeper in the selectivity filter may induce different degrees of structural 'deformation' at external ion binding sites. Similar observations that internal ions can influence putative external binding sites have been made in Kv2.1 and ROMK1 channels (Immke *et al.* 1999; Spassova & Lu, 1999). As for the residues contributing to the external site, it seems that the position equivalent to threonine (T) 449 in the outer pore mouth of *Shaker* is a key site for regulation of C-type inactivation (Lopez-Barneo *et al.* 1993). Mutations at this position that alter inactivation of other K^+ channels also change modulation by K_o^+ (Pardo *et al.* 1992; Kirsch *et al.* 1992; Lopez-Barneo *et al.* 1993). For example, replacement of T449 of a mutant *Shaker* B channel (ShBΔ6–46) with lysine or glutamate increased the rate of C-type inactivation 100-fold and made the channel availability sensitive to K_o^+ (Lopez-Barneo *et al.* 1993). Similarly, in Kv1.4, mutation of a single amino acid (K533Y) in a position homologous to T449 abolished K_o^+ modulation of these channels (Pardo *et al.* 1992). In HERG, strong effects of mutations at S631 (equivalent to T449 in *Shaker*) on inactivation have been reported (Smith *et al.* 1996; Schönherr & Heinemann, 1996). Mutation of serine 631 to alanine (S631A) also caused a dramatic shift in the voltage dependence of channel inactivation, but, reflecting the results reported here, did not affect the voltage dependence of activation (Zou *et al.* 1998). However, increasing extracellular K^+ still slowed inactivation in HERG S631A mutant channels (Zou *et al.* 1998). Therefore, the binding site(s) at which K_o^+ and Cs_o^+ regulate inactivation is not known.

Implications for the molecular basis of HERG inactivation

Unlike C-type inactivation in *Shaker* channels, HERG inactivation is strongly voltage dependent and so the channel has been suggested to possess an independent voltage sensor (Wang *et al.* 1996; Johnson *et al.* 1999). However, Baukrowitz & Yellen (1996) proposed that in *Shaker* channels K^+ ions controlled the C-type inactivation rate at a K^+ binding site involved in permeation, and that it was the off-rate of the last ion from a binding site in the permeation pathway that controlled the inactivation rate (Baukrowitz & Yellen, 1996). From studies of chimeric Kv2.1/1.3 channels Kiss & Korn (1998) proposed a model in which the selectivity filter binding site is the primary site at which K^+ modulates inactivation, such that C-type inactivation involves a constriction at the selectivity filter, and the constriction cannot proceed when the selectivity filter is occupied by K^+. Our results on HERG channels suggest that Cs_o^+ not only slows inactivation, but also modulates the voltage sensitivity of the τ_{inact}–V relationship by binding to a site in the pore. This suggests that ion and channel interactions also contribute to the voltage dependence of HERG inactivation as is the case for Kv channels. However, the contribution of external cations to the voltage dependence (which, in terms of our model, depends on $K_d(0)$ and δ) is less important than the 'intrinsic' voltage dependence ($Z'\delta'$) because the external ion effect is rather small under physiological conditions. Our model does not explicitly consider effects of occupancy by internal cations. However, our results showed that there are clear differences in gating kinetics between Cs^+- and K^+-mediated current.

Conclusions

Raising the external Cs^+ concentration dramatically slows HERG channel inactivation, but does not affect HERG activation properties. Cs_o^+ increases τ_{inact} and modulates the voltage sensitivity of τ_{inact}. Both effects are concentration dependent and well described by a simple model in which binding of Cs_o^+ or K_o^+ slows HERG inactivation in a voltage-dependent manner. Although the site interacts with K^+ and Cs^+ similarly, the apparent electrical location appears to depend on the nature of the internal cation. The strong effects of permeant ions on inactivation but not on activation suggest that permeant ion and channel interactions contribute significantly to HERG inactivation properties.

REFERENCES

Barros F, Gomez-Varela D, Viloria CG, Palomero T, Giraldez T & De la Peña P (1998). Modulation of human erg K^+ channel gating by activation of a G protein coupled receptor and protein kinase C. *J Physiol* **511**, 333–346.

Baukrowitz T & Yellen G (1995). Modulation of K^+ current by frequency and external $[K^+]$: A tale of two inactivation mechanisms. *Neuron* **15**, 951–960.

Baukrowitz T & Yellen G (1996). Use-dependent blockers and exit rate of the last ion from the multi-ion pore of a K^+ channel. *Science* **271**, 653–656.

Bianchi L, Wible B, Arcangeli A, Taglialatela M, Morra F, Castaldo P, Crociani O, Rosati B, Faravelli L, Olivotto M & Wanke E (1998). HERG encodes a K^+ current highly conserved in tumors of different histogenesis – a selective advantage for cancer cells. *Cancer Res* **58**, 815–822.

Faravelli L, Arcangeli A, Olivotto M & Wanke E (1996). A HERG-like K^+ channel in rat F-11 DRG cell line: Pharmacological identification and biophysical characterization. *J Physiol* **496**, 13–23.

Fedida D, Maruoka ND & Lin S (1999). Modulation of slow inactivation in human cardiac Kv1.5 channels by extra- and intracellular permeant cations. *J Physiol* **515**, 315–329.

Hille B (2001). Ion selectivity. In *Ion Channels of Excitable Membranes*, 3rd edn, p. 21. Sinauer Associates, Sunderland, MA, USA.

Hoshi T, Zagotta WN & Aldrich RW (1991). Two types of inactivation in *Shaker* K^+ channels: Effects of alterations in the carboxy-terminal region. *Neuron* **7**, 547–556.

Immke D, Wood M, Kiss L & Korn SJ (1999). Potassium-dependent changes in the conformation of the Kv2.1 potassium channel pore. *J Gen Physiol* **113**, 819–836.

Johnson JP Jr, Mullins FM & Bennett PB (1999). Human *ether-à-go-go*-related gene K^+ channel gating probed with extracellular Ca^{2+}. Evidence for two distinct voltage sensors. *J Gen Physiol* **113**, 565–580.

Kirsch GE, Drewe JA, Taglialatela M, Joho RH, Debiasi M, Hartmann HA & Brown AM (1992). A single nonpolar residue in the deep pore of related K^+ channels acts as a K^+:Rb^+ conductance switch. *Biophys J* **62**, 136–144.

Kiss L & Korn SJ (1998). Modulation of C-type inactivation by K^+ at the potassium channel selectivity filter. *Biophys J* **74**, 1840–1849.

Lopez-Barneo J, Hoshi T, Heinemann SH & Aldrich RW (1993). Effects of external cations and mutations in the pore region on C-type inactivation of Shaker potassium channels. *Receptors & Channels* **1**, 61–71.

Matteson DR & Swenson RP (1986). External monovalent cations that impede the closing of K^+ channels. *J Gen Physiol* **87**, 795–816.

Numaguchi H, Mullins FM, Johnson JP Jr, Johns DC, Po SS, Yang IC, Tomaselli GF & Balser JR (2000). Probing the interaction between inactivation gating and D-sotalol block of HERG. *Circ Res* **87**, 1012–1018.

Ogielska EM, Zagotta WN, Hoshi T, Heinemann SH, Haab J & Aldrich RW (1995). Cooperative subunit interactions in C-type inactivation of K channels. *Biophys J* **69**, 2449–2457.

Pancrazio JJ, Ma W, Grant GM, Shaffer KM, Kao WY, Liu QY, Manos P, Barker JL & Stenger DA (1999). A role for inwardly rectifying K^+ channels in differentiation of NG108–15 neuroblastoma x glioma cells. *J Neurobiol* **38**, 466–474.

Pardo LA, Heinemann SH, Terlau H, Ludewig U, Lorra C, Pongs O & Stühmer W (1992). Extracellular K^+ specifically modulates a rat brain K^+ channel. *Proc Natl Acad Sci U S A* **89**, 2466–2470.

Pennefather PS, Zhou W & DeCoursey TE (1998). Idiosyncratic gating of HERG-like K^+ channels in microglia. *J Gen Physiol* **111**, 795–805.

Ruben P & Thompson S (1984). Rapid recovery from K current inactivation on membrane hyperpolarization in molluscan neurons. *J Gen Physiol* **84**, 861–875.

Sanguinetti MC, Jiang C, Curran ME & Keating MT (1995). A mechanistic link between an inherited and an acquired cardiac arrhythmia: HERG encodes the I_{Kr} potassium channel. *Cell* **81**, 299–307.

Sanguinetti MC & Jurkiewicz NK (1990). Two components of delayed rectifier K^+ current. *J Gen Physiol* **96**, 195–215.

Schönherr R & Heinemann SH (1996). Molecular determinants for activation and inactivation of HERG, a human inward rectifier potassium channel. *J Physiol* **493**, 635–642.

Smith PL, Baukrowitz T & Yellen G (1996). The inward rectification mechanism of the HERG cardiac potassium channel. *Nature* **379**, 833–836.

Spassova M & Lu Z (1999). Tuning the voltage dependence of tetraethylammonium block with permeant ions in an inward-rectifier K^+ channel. *J Gen Physiol* **114**, 415–426.

Spector PS, Curran ME, Zou AR & Sanguinetti MC (1996). Fast inactivation causes rectification of the I_{Kr} channel. *J Gen Physiol* **107**, 611–619.

Swenson RP & Armstrong CM (1981). K^+ channels close more slowly in the presence of external K^+ and Rb^+. *Nature* **291**, 427–429.

Trudeau MC, Warmke JW, Ganetzky B & Robertson GA (1995). HERG, a human inward rectifier in the voltage-gated potassium channel family. *Science* **269**, 92–95.

Wang S, Liu S, Morales MJ, Strauss HC & Rasmusson RL (1997). A quantitative analysis of the activation and inactivation kinetics of *HERG* expressed in *Xenopus* oocytes. *J Physiol* **502**, 45–60.

Wang S, Morales MJ, Liu S, Strauss HC & Rasmusson RL (1996). Time, voltage and ionic concentration dependence of rectification of h-erg expressed in *Xenopus* oocytes. *FEBS Lett* **389**, 167–173.

Woodhull AM (1973). Ionic blockage of sodium channels in nerve. *J Gen Physiol* **61**, 687–708.

Zhang S, Rajamani S, Chen Y, Gong Q, Rong Y, Zhou Z, Ruoho A & January CT (2001). Cocaine blocks HERG, but not KvLQT1+minK, potassium channels. *Mol Pharmacol* **59**, 1069–1076.

Zhang S, Zhou Z, Gong Q, Makielski JC & January CT (1999). Mechanism of block and identification of the verapamil binding domain to HERG potassium channels. *Circ Res* **84**, 989–998.

Zhou Y & MacKinnon R (2002). Rate theory from Brownian dynamics: analysis of a simulated ion channel (abstract). *Biophys J* **82**, 350.

Zou A, Xu Q & Sanguinetti MC (1998). A mutation in the pore region of HERG K^+ channels expressed in *Xenopus* oocytes reduces rectification by shifting the voltage dependence of inactivation. *J Physiol* **509**, 129–137.

Acknowledgements

We thank Dr Zhuren Wang for helpful discussions and Sandy Wang and Linda Sui for preparing cells. The project was supported by grants from the Heart and Stroke Foundations of British Columbia and Yukon, and the CIHR to D.F. and a Heart and Stroke Foundation of Canada Research Fellowship Award to S.Z.